



Trans. Nonferrous Met. Soc. China 30(2020) 2764-2774

Transactions of Nonferrous Metals Society of China

www.tnmsc.cn



Design of best performing hexagonal shaped Ag@CoS/rGO nanocomposite electrode material for electrochemical supercapacitor application

Alagu Segar DEEPI, Arputharaj Samson NESARAJ

Department of Applied Chemistry, School of Sciences, Arts, Media and Management, Karunya Institute of Technology and Sciences (Deemed to be University), Karunya Nagar, Coimbatore-641 114, Tamil Nadu, India

Received 10 February 2020; accepted 4 August 2020

Abstract: The mixed metal/metal sulphide (Ag@CoS) with reduced graphene oxide (rGO) nanocomposite (Ag@CoS/rGO) was synthesized for the possible electrode in supercapacitors. Ag@CoS was successfully deposited on the rGO nanosheets by hydrothermal method, implying the growth of 2D Ag and CoS-based hexagonal-like structure on the rGO framework. The synthesized nanocomposite was subjected to structural, morphological and electrochemical studies. The XRD results show that the prepared nanocomposite material exhibits a combination of hexagonal and cubic phase due to the presence of CoS and Ag phases together. The band appearing at nearly 470.33 cm⁻¹ in FTIR spectra can be ascribed to the absorption of S—S bond in the Ag@CoS/rGO nanocomposite. The clear hexagonal structure was analysed by SEM and TEM with the grain sizes ranging from nanometer to micrometer. The electrode material exhibits excellent cyclic stability with a specific capacitance of 1580 F/g at a current density of 0.5 A/g without any loss of capacitive retention even after 1000 cycles. Based on the electrochemical performance, it can be inferred that the prepared novel nanocomposite material is very suitable for using as an electrode for electrochemical supercapacitor applications.

Key words: Ag@CoS/rGO electrode; hydrothermal reaction; physicochemical characteristics; electrochemical performance; electrochemical supercapacitor

1 Introduction

The degrading of fossil fuels and enhancing of global warming are demanding the requirement of effective, clean and best-performing energy storage/conversion devices to meet the greater energy requirements of the globe in the present scenario. Some of the major energy storage devices are batteries, capacitors and fuel cells. The capacitor with known capacitance can stock the electrical charge between its plates, which is proportional to the applied voltage. However, capacitor does not own greater energy density like a battery because it cannot store much energy when

compared to a battery. Battery can store energy but it lacks in discharging rates. Fuel cell requires constant energy input for its mechanism and also it is not economical [1–3]. Being a sustainable energy storage device, supercapacitor aids the gap between conventional capacitors and batteries because of its fair energy density, excellent power density and good cycle life, rapid charging and discharging rates [4]. Taking the charge storage mechanism into consideration, supercapacitors are grouped into three different categories. Electric double-layer capacitor (EDLC), when the electrode material is composed of carbon based materials such as CNT, activated carbon, graphene/graphene derivatives, shows low specific capacitance and the capacitance

of EDLC emerges from the electrode/electrolyte interface [5–9]. Pseudocapacitor includes metal oxides, metal sulphides, metal nitrides, metal hydroxides and conducting polymers. The capacitance of the pseudocapacitor arises due to the Faradic reaction at the electrode/electrolyte interface. Hybrid supercapacitor exhibits both EDLC and pseudocapacitive behaviours. Electrode material makes a major contribution to the functioning of supercapacitors. A wide range of electrode materials, either a single material or composite material, have been used to improve the specific capacitance [9–12].

Metal sulphides like cobalt sulphide and nickel sulphide have captivated immense attention because of their greater specific capacitance, high electrical conductivity, good stability and low cost. These metal sulphides have specific capacitance two times of their metal hydroxides and metal oxide counterparts [13-16]. The increase in capacitance of metal sulphide is due to the replacement of lower electronegative oxygen with sulphur [17,18]. As like metal oxides and metal sulphides, metal tungstates and molybdates have also gained much attention in recent times due to their excellent conductivity and thermal stability [19-21]. Among various transition metal sulphides, cobalt sulphide has gained greater recognition due to its good electrical conductivity, reasonable cost, low toxic level and easy fabrication. The stoichiometric forms and stable crystal structures of cobalt sulphide are CoS, CoS₂, Co₃S₄ and Co₉S₈. Porous nature and rough structure are some of their physical characteristics which support the diffusion of ions in the charge-discharge mechanism. However, cobalt sulphide has high specific capacitance and excelling rate capabilities in the case supercapacitor applications. It is challenging to accomplish the entire objective concurrently by cobalt sulphide itself [22-27]. So, the hybridization of mixed composite material is required. The additional progression of decorating graphene with nanoparticles tunes the quality of nanocomposite and also supports in preventing the loss of surface area that usually occurs because of restacking of the graphene sheets [28]. The combination of cobalt sulphides with graphene/graphene derivatives helps in speedy transportation of ions and electrons to develop the specific capacitance. In addition, it has a large specific area, good physiochemical stability, lightweight and porous Hence. structure. graphene/graphene derivatives have become ideal substructure materials in the preparation of metal sulphide@graphene composite. Among various graphene/graphene derivatives, reduced graphene oxide (rGO) is a widely known two-dimensional material having carbon atoms of sp² hybridization with encouraging mechanical, thermal and chemical stability. For instance, AASHISH et al [29] prepared CoS₂@GONFS through simple route employing rGO as a supporting material with a specific capacitance of 635.8 F/g at 1 A/g in 6 mol/L KOH, which is much greater than that of bare cobalt sulphide. On the other hand, it also shows exceptional cycling performance with 95.4% capacity retention for 2000 cycles.

Some of the nanostructured metals like copper, silver and gold are prominent materials for the catalytic applications, cell separations, cytotoxicity, targeting therapy, energy storage devices and optoelectronic devices because of their intrinsic such as size. properties shape and nanoparticles, being highly conductive, have noteworthy physiochemical and electrochemical properties which include high chemical stability, catalytic activity and reasonable cost. Incorporating silver nanoparticles can enhance the electrical conductivity of electrode materials for energy storage applications [30–32]. Some of the previously reported pieces of literatures for cobalt based materials with different composite combinations like Co_3O_4 (378 F/g), $CoWO_4$ (378 F/g) resulted in a good capacitance with greater rate stability [33,34].

In the present study, a novel Ag@CoS/rGO nanocomposite material was synthesized through hydrothermal method using cobalt nitrate, silver nitrate as precursor salts, thiourea as a sulphur source and acetic acid. The presence of nano-scale CoS particles was expected to greatly enhance the redox activity of the resulting composites as a result of the increased surface area. The obtained Ag@CoS/rGO nanocomposite was examined in a 1 mol/L H₂SO₄ electrolyte solution for electrochemical studies. From the obtained results, it was obvious that the electrode material exhibits a good specific capacitance of 1580 F/g at a current density of 0.5 A/g with high cyclic stability. Owing to its satisfactory specific capacitance, the prepared electrode material may be useful as an outstanding potential candidate for supercapacitor application.

2 Experimental

2.1 Chemicals and materials

The chemicals of cobalt(II) nitrate (99%, Merck, India), silver nitrate (97%, Merck, India), sulphuric acid (97%, Merck, India), thiourea (99%, Rankem, India), acetic acid (90%−100%, Emplura, India), graphite (≥97%, Merck, India), potassium permanganate (97%, Merck, India), ethanol (99.9%, Changshu, Yangyuan, China), N-methyl-2-pyrrolidone (NMP) (99%, Sigma, India), hydrochloric acid (97%, Merck, India), hydrogen peroxide (30%, Merck, India) and polyvinylidene fluoride (PVDF) (Sigma, India) were used in this experiment without any further purification.

2.2 Synthesis of Ag/CoS/rGO nanocomposite

As reported in Ref. [35] the modified Hummer's method was handled to synthesize graphene oxide. Primitively, the equal molar ratio (1:1) of cobalt nitrate (0.914 g) and silver nitrate (0.849 g) were dissolved in double distilled water (50 mL) containing dispersed graphene oxide (25 mg). The afore-mentioned solution was stirred and ultrasonicated for about 0.5 h. To this solution 0.7 mol/L thiourea (CH₄N₂S; 2.6642 g) and 0.2 mol/L acetic acid (2.5 mL approx.) were mixed. The overall mixed solution was sealed in a Teflon autoclave and retained at 180 °C for 24 h. It is known that the size of the nanoparticles must be controlled in appropriate nucleation period, and the final particle number does not change in that time. The resulted composite was filtered, washed out and kept in a vacuum oven at 60 °C to obtain a pure Ag@CoS/rGO nanocomposite material. The temperature and other experimental conditions induced in the precursor solution during the hydrothermal reaction provided the energy required for the formation of the CoS nuclei in the Ag@CoS/rGO. The mechanism of the reaction process can be explained based on reactions shown Eqs. (1) and (2):

Step 1: Stirring and ultra-sonication

 $Co(NO_3)_2 + AgNO_3 + rGO \rightarrow$

Metal nitrates@rGO composite (1)

Step 2: Hydrothermal reaction

Metal nitrates@rGO composite+

$$CH_4N_2S$$
 (thiourea)+ $CH_3COOH \rightarrow$
Ag@CoS/rGO nanocomposite (2)

In the first step, the nitrate solutions were mixed thoroughly with rGO in ultra-sonication process. This may result in the formation of metal nitrate@rGO composite. In the next step, the as-formed metal nitrates@rGO composite was treated with thiourea and acetic acid via hydrothermal reaction at 180 °C for a prolonged duration (24 h). During this process, silver nitrate reacted with acetic acid, which resulted as silver acetate and then decomposed to silver nanoparticles at 180 °C for 24 h as reported in Ref. [36]. The cobalt nitrate reacted with thiourea and resulted as hierarchicalcobalt sulphide during the hydrothermal reaction carried out at 180 °C for 24 h as reported in Ref. [36]. As a result, Ag@CoS/rGo nanocomposite was formed. The unwanted impurities were washed out with the mixture of water and ethanol (9:1, volume ratio).

2.3 Fabrication of working electrode

0.5 mg of the prepared material was coated on the surface of a thin graphite sheet (1 cm × 1 cm) which acted as a conducting substrate. Before coating, the as-prepared electrode material was well mixed with N-methyl-2-pyrrolidine (NMP) with the addition of PVDF as a binder and stirred well for 16–20 h. Then, the well-blended solution was dried at 70 °C for about 1 h to remove the organic matters and coated on the above thin graphite sheet [37].

2.4 Material characterization

The crystal structure and properties were studied by an XRD6000 X-ray diffractometer (Shimadzu, Japan) using Cu K_{α} radiation. An IR Prestige–21 model FTIR spectrometer (Shimadzu, Japan) in the range of 4000–400 cm⁻¹ was used to identify chemical molecules present in the sample. The surface microstructural studies were carried out by a JEOL Model JSM–6360 scanning electron microscope. The TEM studies were done by HRTEM-JEOL JEM 2100 instruments. A JEOL Model JSM–6360 was employed to check the elemental composition in the sample (EDAX analysis).

An electrochemical workstation (Model CH1660C) attached to the three-electrode system was utilized to study the electrochemical analysis. Ag@CoS/rGO was used as a working electrode;

whereas the saturated calomel electrode (SCE) and platinum electrode were used as the reference and counter electrodes, respectively.

3 Results and discussion

3.1 XRD pattern

The XRD pattern for the mixed composite of Ag@CoS/rGO nanoparticles using thiourea as a sulphur source is shown in Fig. 1. The highly intense and well defined sharp peaks were spotted at 2θ values of 31.27° (101), 34.23° (222) and 36.51° (111), respectively. Interestingly, diffraction peaks appearing at 2θ values of 31.27° , 25.89° , 28.70°, 40.46°, 45.90°, 53.15° and 69.67° which respectively correlated with planes (101), (211), (220), (331), (333), (440) and (620) describe the face-centered cubic CoS phase. The obtained peak diffraction and interplanar spacing correspond to the standard diffraction pattern of primitive hexagonal CoS phase (JCPDS No. 75-0605) [38-43]. The obtained XRD pattern of CoS in Ag@CoS/rGO nanocomposite has matched with the above JCPDS data for CoS phase. CoS in the nanocomposite is indexed to a pure hexagonal phase of CoS as reported in Ref. [36]. No other impurities are detected, which shows the high purity of the product (CoS). Additionally, the sharp peaks indicate that the product is well crystallized.

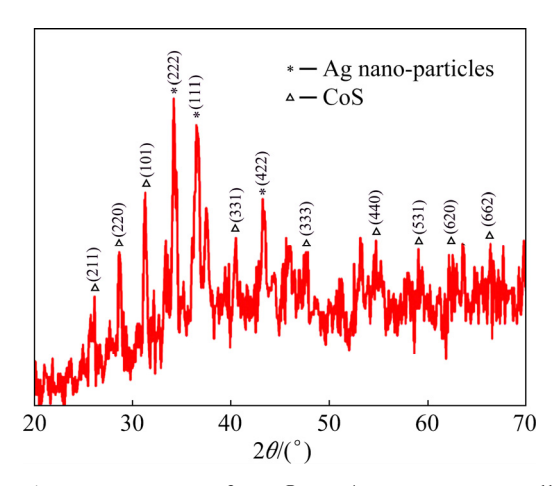


Fig. 1 XRD pattern of Ag@CoS/rGO nano-crystalline electrode material

The presence of Ag in Ag@CoS/rGO is confirmed with the appearance of a strong diffraction peak at 2θ =36.51° as reported in JCPDS No. 04–0783 for Ag. The appearance of Ag peak is

indicated with an asterisk in Fig. 1. The XRD pattern of Ag is assigned as a single phase of metallic Ag with the cubic crystal structure as reported. In the reaction temperature range, no crystalline intermediate phase can be identified, indicating the formation of metallic Ag directly by the thermal decomposition of silver acetate as reported in Ref. [35]. Additionally, it should be emphasized that it is challenging to accomplish pure cobalt–sulphide phase of Co_mS_n resulting from the complex stoichiometry of various cobalt sulphides. The rGO peaks were witnessed in the mixed-phase but it was overlapped owing to high loading mass of Ag and CoS mixtures. From above, it is confirmed that Ag@CoS/rGO composite has Ag, CoS and rGO phases.

The average crystalline size (D) for the nanocomposite material was evaluated by Scherrer equation (Eq. (3))

$$D = K\lambda/(\beta \cos \theta) \tag{3}$$

where K is the Scherrer's constant; λ is the X-ray wavelength; β is the full width at half maximum intensity of the peak; θ is the Bragg's angle.

From Eq. (3), the obtained crystalline size *D* was 2.4 nm that is very close to the *d*-spacing value (2.9 nm). No impurity peaks are found in the sample. From the study, it is evident that the prepared mixed nanocomposite is a well-mixed phase pure electrode material.

3.2 FTIR spectrum

To investigate the chemical bonding behaviour and to check whether the particle surface is capped with organic material, the FTIR study was carried out. The FTIR spectrum of the mixed composite material obtained from the synthesized Ag@CoS/ rGO is shown in Fig. 2. The band appearing at nearly 470.33 cm⁻¹ could be ascribed to the absorption of S—S bond in the Ag@CoS/rGO. The presence of a band at 599.86 cm⁻¹ corresponds to the silver. The band at 873.75 cm⁻¹ may be assigned to $-CH_2$ in the sample. The band at 1147 cm⁻¹ is due to the presence of C-C and C-O-C in the cobalt-sulphide nanocomposite material. The bands observed at 1517.98 and 3435.22 cm⁻¹ were reserved to the aromatic group containing weak stretching vibration in the graphene sheets, which signify the reduction of GO and recovery of the conjugated aromatic system and the absorption of H₂O molecules in the sample, respectively [43,44].

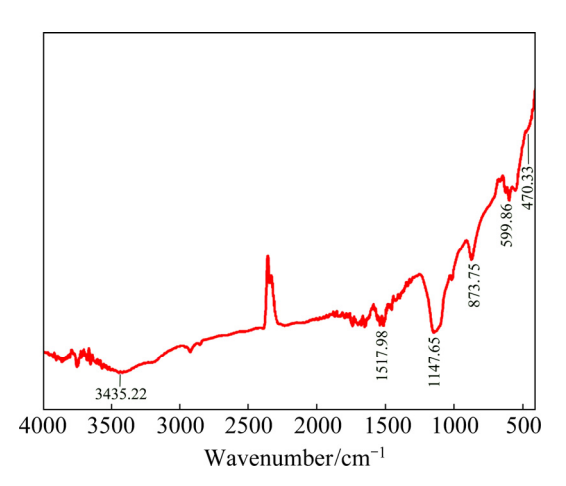


Fig. 2 FTIR spectrum of Ag@CoS/rGO nano-crystalline electrode material

3.3 Surface morphology

To study the surface morphology of the nanocomposite material SEM was examined. The SEM images of hexagonal-shaped Ag@CoS/rGO nanocrystalline electrode material are presented in Fig. 3. The resulted product after 24 h of hydrothermal reaction depicts the uniform hexagonal structures of CoS with some irregularly broken plates showing the presence of Ag nanoparticles on the surface or the rGO nanosheets. The hexagonal structure is composed of cobalt and

sulphur elements with a molar ratio of 1:1. The obtained surface morphology exhibits high surface area which accesses to the electrolyte, results in the considerable improvement in the specific capacitance and simultaneously reduces the electron transfer resistance. The SEM images in Fig. 3 provide evidence that the nanocomposite is amorphous, which is caused by the bond between cobalt and sulphur and the hexagonal structure shown in Fig. 3(b) is in agreement with XRD analysis. SEM images confirm the presence of grains in the size range from nanometer to micrometer in the sample. Furthermore, to visualize the microstructure of the prepared composite material HRTEM images were studied. Figures 4(a, b) evidently show the presence of graphene sheet in the sample. Figure 4(c) indicates the merging of cluster upon the surface of a graphene sheet, which reveals that the nanocomposite is well wrapped with the graphene sheet. The crystallinity nature of the composite material is confirmed from Fig. 4(d), which is reconfirmed through the SAED pattern (Figs. 4(e) and (f)). According to the available data, this is the first ever report showing the presence of singlecrystalline and poly-crystalline behaviour resulted from the appearance of CoS and Ag nanoparticles,

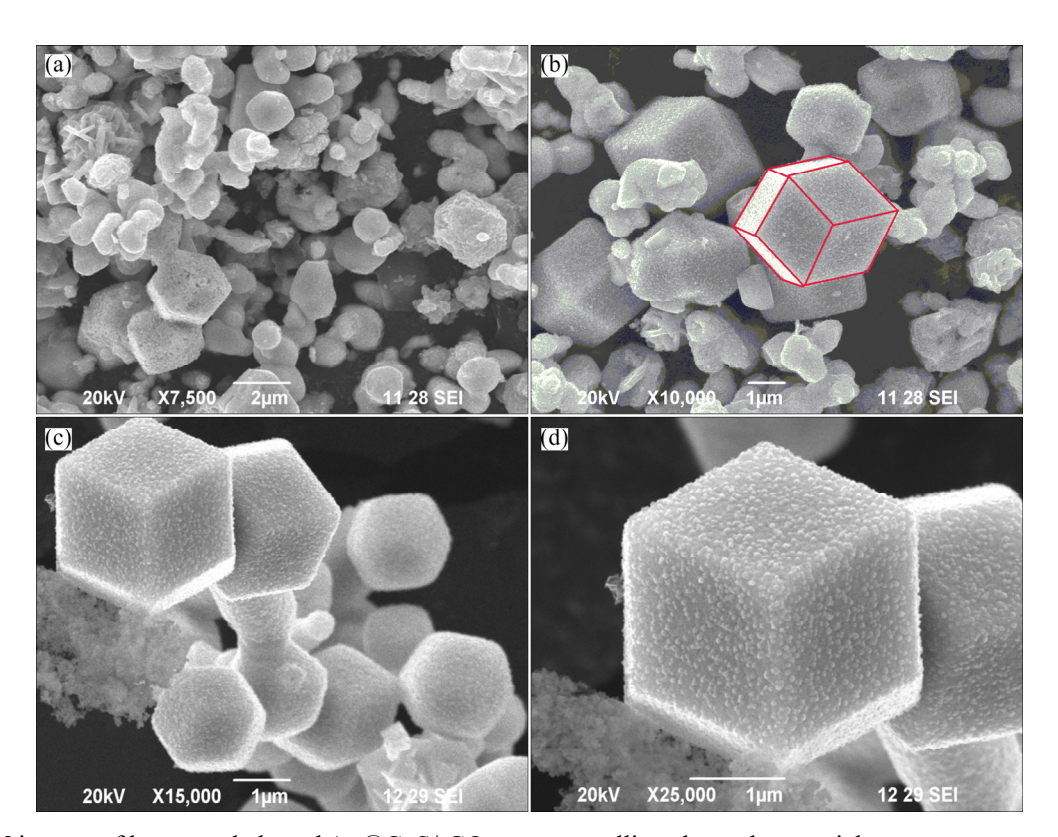


Fig. 3 SEM images of hexagonal-shaped Ag@CoS/rGO nano-crystalline electrode material

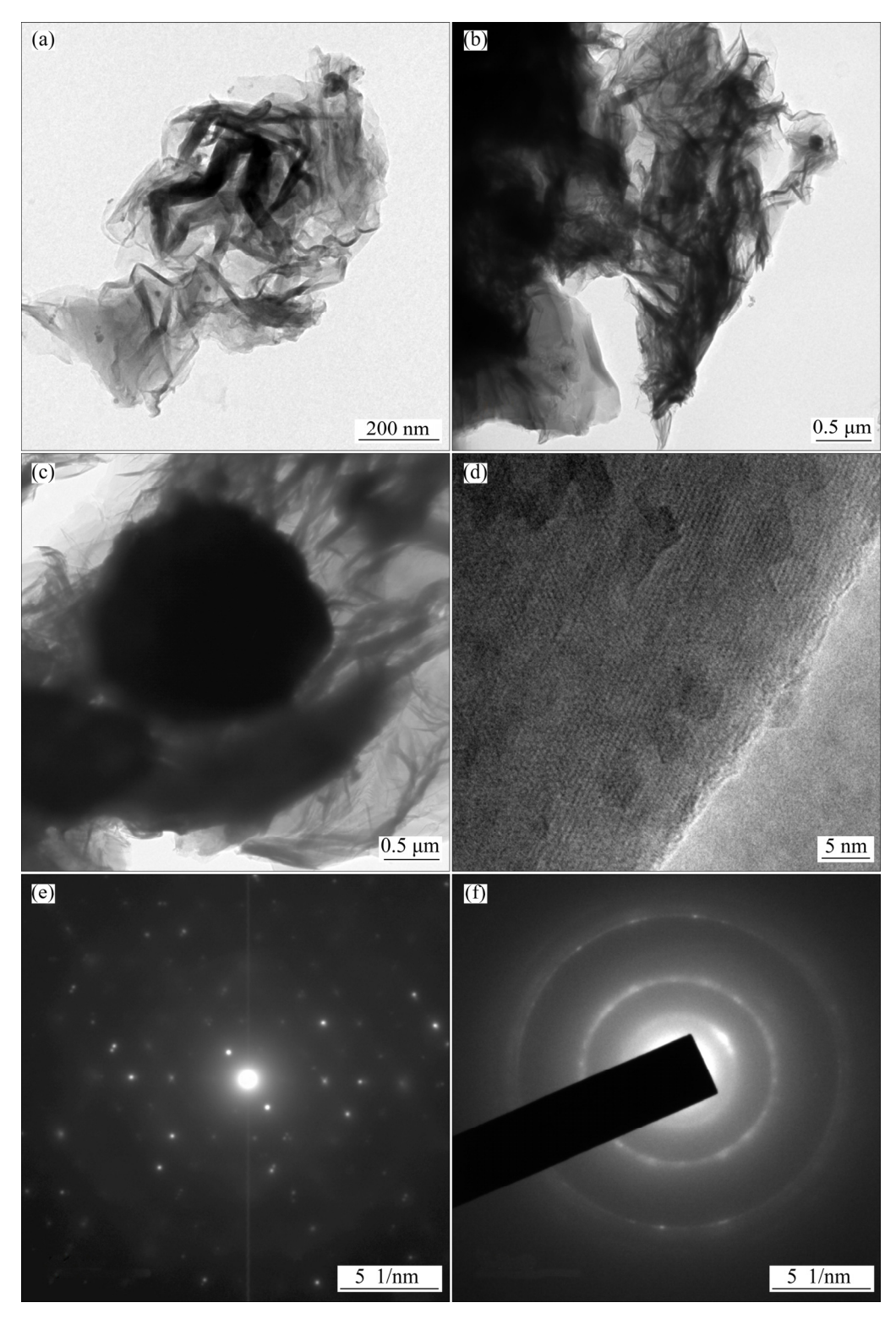


Fig. 4 HRTEM images of Ag@CoS/rGO nano-crystalline electrode material: (a, b) Clear images of graphene in sample; (c) Presence of Ag@CoS/rGO on surface of graphene sheet; (d) Lattice fringes of sample; (e, f) SAED patterns of single-crystalline and poly-crystalline of Ag@CoS/rGO, respectively

respectively. This is also a justification for the high specific capacitance and capacitive retention that turn out to be a promising cathode material for supercapacitor application.

3.4 EDAX spectrum

The elemental composition of the synthesized mixed nanocomposite electrode material was evaluated by EDAX analysis and the resulted

EDAX spectrum is shown in Fig. 5. The mass and molar fractions of the elements are shown in Table 1. From the obtained data, sulphur content is fairly high in terms of both the mass and molar fractions, indicating the presence of CoS phase.

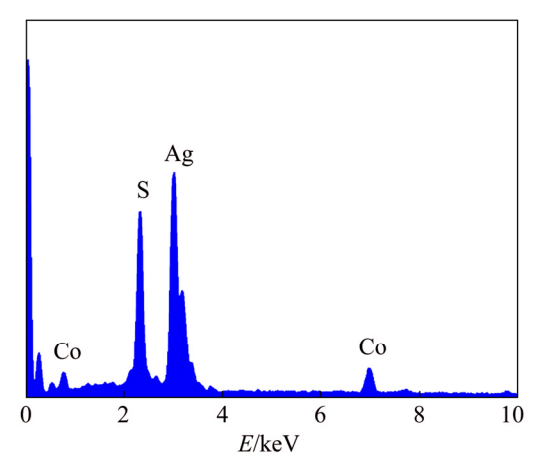


Fig. 5 Energy dispersive analysis (EDAX) spectrum of Ag@CoS/rGO nano-crystalline electrode material

Table 1 EDAX data of Ag@CoS/rGO nanocrystalline electrode material

Element	wt.%	at.%
Со	8.62	10.25
S	19.80	43.26
Ag	71.57	46.48

3.5 Electrochemical properties

Figure 6 represents the CV curves for the mixed nanocomposite material in 1 mol/L H₂SO₄ electrolyte solution at different scan rates ranging from 10 to 100 mV/S with a potential range varying from -0.2 to 0.6 V. The obtained CV curve is in contrast with EDLC behaviour, which shows a quasi-rectangular shape at all the scan rates; whereas the pseudocapacitive behaviour shows an ideal rectangular-shaped curve [45,46]. In this study, it is witnessed that the shape and position of the redox peaks remain unchanged, signifying that there is rapid charging and discharging kinetics in the redox reaction. Meanwhile, the increase in scan rate increases the peak current density. This is due to the exchange of charge in a faradic reaction at the electrode and electrolyte interface. For the reason of increased scan rate, the anode and cathode potentials were found to drift in the positive direction because of the internal diffusion resistance in the cobalt-sulphide composite while increasing

the scan rate. In accordance with the outcome, the mixed nanocomposite Ag@CoS/rGO exhibits the excellent reversibility and the appealing rate capability [47,48]. From the CV curves of Ag@CoS/rGO, it is evident that the charge storage mechanism is the same as ideal capacitance which outlays from the electric double-layer capacitance. The well-specified redox CV curves explicitly show that metal sulphide composite has a faradic charge storage mechanism occurring between the surfaces of electrode and electrolyte [49].

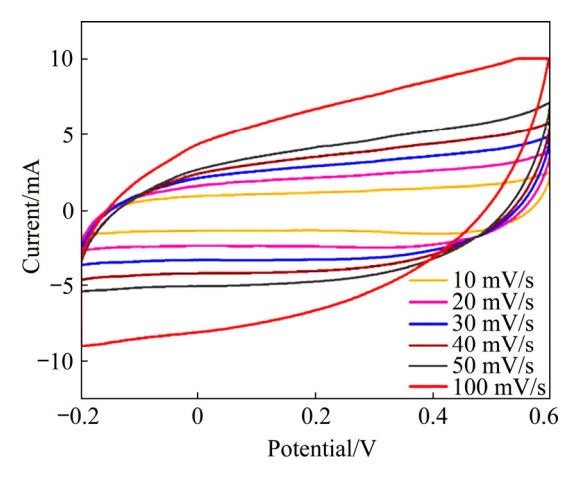
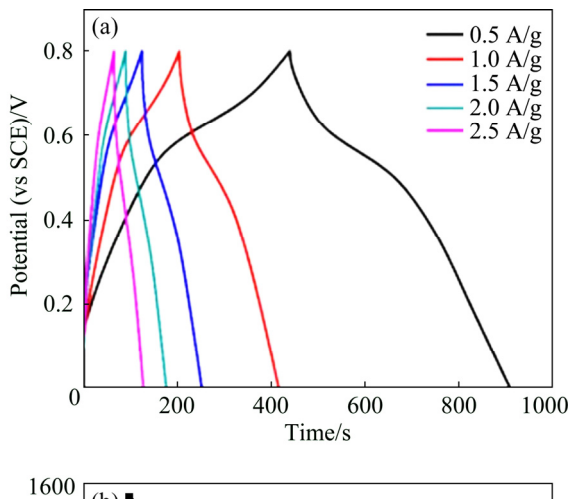


Fig. 6 CV curves of Ag@CoS/rGO electrode material at different scan rates in 1 mol/L H_2SO_4 electrolyte solution in potential range from -0.2 to 0.6 V

Additionally, the charging capacity was evaluated at different current densities altering from 0.5 to 2.5 A/g in 1 mol/L H₂SO₄ solution in a broad range of potential from 0 to 0.8 V. Figure 7(a) shows typical triangle-shaped curves which reveal the ideal capacitive behaviour followed by the reversible faradic process inferring the charge storage mechanism. At higher current density, the specific capacitance is lowered as a result of a slower faradic reaction between the electroactive ions from the electrolyte and electrode [50-53]. In addition, the charge-discharge curve has less voltage drop during the discharging process, showing that the ternary transition metal sulphide has excellent ionic and electrical conductivity. From the following equation (Eq. (4)), the specific capacitance can be measured.

$$C_{\rm s} = \frac{I\Delta t}{m\Delta V} \tag{4}$$

where C_s is the specific capacitance of the electrode material (F/g), I is the discharge current (A), Δt is



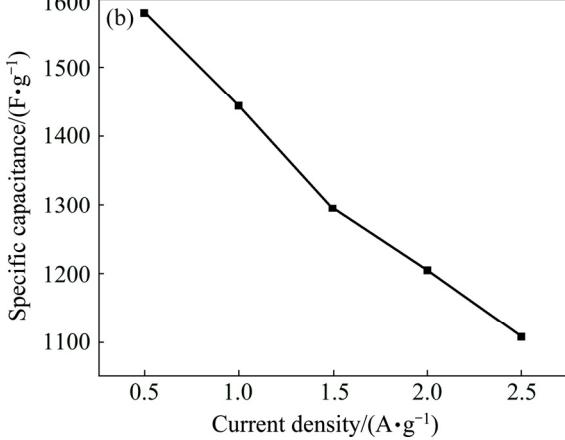


Fig. 7 Galvanostatic charge/discharge curves of Ag@CoS/rGO electrode material at various current densities in 1 mol/L H₂SO₄ electrolyte medium (a) and specific capacitance of Ag@CoS/rGO electrode material at various current densities (b)

the discharge time (s), m is the mass of the loaded electro-active material (g) and ΔV is the operating voltage window (V). The Ag@CoS/rGO material proclaimed specific capacitances of 1580, 1443, 1295, 1204 and 1108 F/g at varying current densities of 0.5, 1.0, 1.5, 2.0 and 2.5 A/g shown in Fig. 7(b), respectively. The fabricated electrode showed the highest specific capacitance of 1580 F/g owing to its higher surface morphology and electron transfer efficiency.

The fabricated electrode material was subjected to the electrochemical impedance spectroscopy to understand the conductivity and ion transfer. Figure 8 shows the Nyquist plot of the electrode with a semi-circle in a lower frequency region denoting the charge transfer resistance ($R_{\rm ct}$) and a steep linear spike in a high-frequency region suggesting the ideal capacitive behaviour. The Warburg resistance at an angle of 45° refers to the

controlled diffusion at the electrode/electrolyte interface. The insert in Fig. 8 specifies the equivalent circuit, which holds the parameters of solution resistance (R_1) , particle resistance (R_2) , Warburg open resistance (W_1) and constant phase element (CPE₁). The intrinsic electrode resistance and contact resistance were limited by the positioning of Ag nanoparticles and rGO that sets out vital admittance for the electrolyte/electrode interface. According to the impedance data, it is cogently confirmed that the Ag@CoS/rGO composite imparts predominance in ion transfer and electrochemical kinetics [45–46,54].

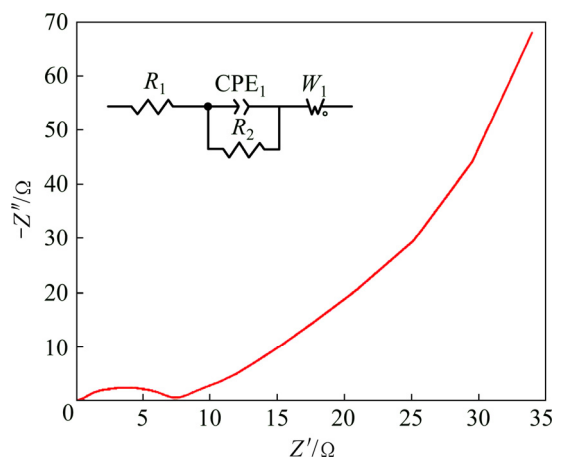


Fig. 8 Nyquist plot of Ag@CoS/rGO electrode measured in frequency range of 1–10⁵ Hz at scan rate of 5 mV/s

To highlight the long-term stability of prepared electrode material, capacitive retention study was carried out using cyclic voltammetry at a scan rate of 10 mV/s for 1000 cycles. The capacity retention curve of Ag@CoS/rGO electrode materials by cyclic voltammetry is shown in Fig. 9. Figure 9

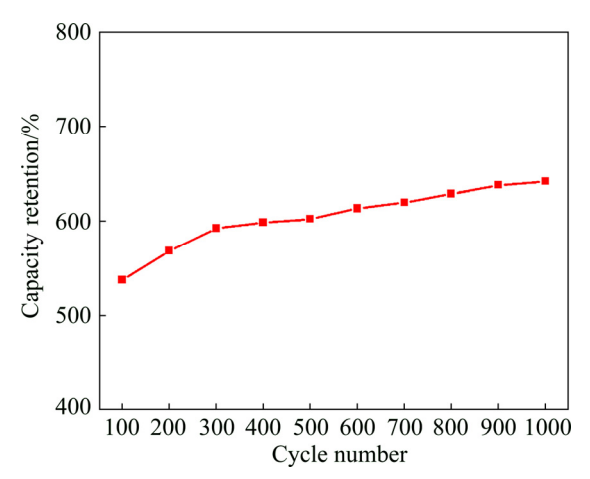


Fig. 9 Capacity retention curve of Ag@CoS/rGO electrode material obtained by cyclic voltammetry

shows a gradual increase in the capacitance without any loss. This is due to the piercing of ions into the electrode from the electrolyte, which helps in activating more electroactive ions within the electrode. The cyclic stability of Ag@CoS/rGO favors electrochemical stability, which makes it a promising electrode material for supercapacitor.

4 Conclusions

- (1) The Ag@CoS/rGO nanocomposite electrode material was synthesized by the hydrothermal supercapacitor method applications.
- (2) The physical characterization of the sample shows the presence of cobalt-sulphide phase with both single-crystalline and polyhexagonal structures.
- (3) Ag@CoS/rGO nanocomposite exhibits good electrochemical performance with a specific capacitance of 1580 F/g at a current density of 0.5 A/g, showing superior ion transfer rates and electrochemical kinetics with enhanced performance.
- (4) The prepared Ag@CoS/rGO electrode material possesses good ionic and electrical conductivities with better cycling stability after 1000 cycles. Therefore, Ag@CoS/rGO nanocomposite material may be a potential candidate for electrochemical supercapacitors.

Acknowledgments

The authors would like to thank management of Karunya Institute of Technology and Sciences for promoting "Electrochemical Energy Conversion" based research activity in the Department of Applied Chemistry.

References

- [1] SAHOO S, NAIK K K, LATE D J, ROUT C S. Electrochemical synthesis of a ternary transition metal sulfide nanosheets on nickel foam and energy storage application [J]. Journal of Alloys and Compounds, 2013, 695: 154-161.
- CHOU S W, LIN J Y. Cathodic deposition of flaky nickel sulfide nanostructure as an electroactive material for high-performance supercapacitors [J]. Journal of the Electrochemical Society, 2013, 160: D178-D182.
- HU W, CHEN R, XIE W, ZOU L, QIN N, BAO D. CoNi₂S₄ nanosheet arrays supported on nickel foams with ultrahigh capacitance for aqueous asymmetric supercapacitor

- applications [J]. ACS Applied Materials & Interfaces, 2014, 6: 19318-19326.
- BURKE A. Ultra capacitors: Why, how, and where is the technology [J]. Journal of Power Sources, 2000, 91: 37-50.
- FRACKOWIAK E. Carbon materials for supercapacitor application [J]. Physical Chemistry Chemical Physics, 2007, 9: 1774-1785.
- [6] MILLER J R, SIMON P. Electrochemical capacitors for energy management [J]. Science, 2008, 321: 651-652.
- SIMON P, GOGOTSI Y. Materials for electrochemical capacitors [J]. Nature Materials, 2008, 7: 845-854.
- [8] LEE C, KIM S K, CHANG H. Active electrode materials of graphene balls and their composites for supercapacitors: A perspective view [J]. Advanced Powder Technology, 2019, 30: 3079-3087.
- [9] CHANG W M, WANG C C, CHEN C Y. Fabrication of ultra-thin carbon nanofibers by centrifuged-electrospinning application in high-rate supercapacitors [J]. Electrochimica Acta, 2019, 296: 268-275.
- [10] BROUSSE T, BÉLANGER D, LONG J W. To be or not to be pseudocapacitive? [J]. Journal of the Electrochemical Society, 2015, 162: A5185-A5189.
- [11] WANG H, WANG W, WANG H, LI Y, JIN X, NIU H, WANG H, ZHOU H, LIN T. Improving supercapacitance of electrospun carbon nanofibers through increasing micropores and microporous surface area [J]. Advanced Materials Interfaces, 2019, 6: 180900.
- [12] CHEN S M, RAMACHANDRAN R, MANI V, SARASWATHI R. Recent advancements in electrode materials for the high-performance electrochemical supercapacitors: A review [J]. International Journal of Electrochemical Science, 2014, 9: 4072-4085.
- [13] SHEN L, WANG J, XU G, LI H, DOU H, ZHANG X. NiCo₂S₄ nanosheets grown on nitrogen doped carbon foams as an advanced electrode for supercapacitors [J]. Advanced Energy Materials, 2015, 5: 1400977.
- [14] CHEN H, JIANG J, ZHANG L, WAN H, QIA T, XIA D. Highly conductive NiCo₂S₄ urchin-like nanostructures for high-rate pseudocapacitors [J]. Nanoscale, 2013, 5: 8879-8883.
- [15] XIAO J, WAN L, YANG S, XIAO F, WANG S. Design hierarchical electrodes with highly conductive NiCo2S4 nanotube arrays grown on carbon fiber paper for highperformance pseudocapacitors [J]. Nano Letters, 2014, 14: 831-838.
- [16] XIA C, ALSHAREEF H N. Self-templating scheme for the synthesis of nanostructured transition-metal chalcogenide electrodes for capacitive energy storage [J]. Chemistry of Materials, 2015, 27: 4661-4668.
- [17] TONG H, BAI W, YUE S, GAO Z, LU L, SHEN L, DONG S, ZHU J, HE J, ZHANG X. Zinc cobalt sulfide nanosheets grown on nitrogen-doped graphene/carbon nanotube film as a high-performance electrode for supercapacitors [J]. Journal of Materials Chemistry A, 2016, 4: 11256-11263.
- [18] KULKARNI P, NATARAJ S K, BALAKRISHNA R G, NAGARAJU D H, REDDY M V. Nanostructured binary and ternary metal sulfides: Synthesis methods and their application in energy conversion and storage devices [J]. Journal of Materials Chemistry A, 2017, 5: 22040-22094.

- [19] SOBHANI-NASAB A, RAHIMI-NASRABADI M, NADERI H R, POURMOHAMADIAN V, AHMADI F, GANJALI M R, EHRLICH H. Sonochemical synthesis of terbium tungstate for developing high power supercapacitors with enhanced energy densities [J]. Ultrasonics Sonochemistry, 2018, 45: 189–196.
- [20] SOBHANI-NASAB A, NADERI H, RAHIMI-NASRABADI M, GANJALI M R. Evaluation of supercapacitive behavior of samarium tungstate nanoparticles synthesized via sonochemical method [J]. Journal of Materials Science: Materials in Electronics, 2017, 28: 8588–8595.
- [21] RAHIMI-NASRABADI M, POURMOHAMADIAN V, KARIMI M S, NADERI H R, KARIMI M A, DIDEHBAN K,GANJALI M R. Assessment of supercapacitive performance of europium tungstate nanoparticles prepared via hydrothermal method [J]. Journal of Materials Science: Materials in Electronics, 2017, 28: 12391–12398.
- [22] ZHAO Y P, WANG L, SOUGRATI M T, FENG Z, LECONTE Y, FISHER A, SRINIVASAN M, XU Z. A review on design strategies for carbon based metal oxides and sulphides nanocomposites for high performance Li and Na ion battery anodes [J]. Advanced Energy Materials, 2017, 7: 1601424.
- [23] RANAWEERA C K, WANG Z, ALQURASHI E, KAHOL P K, DVORNIC P R, GUPTA B K, RAMASAMY K, MOHITE A D, GUPTA G, GUPTA R K. Highly stable hollow bifunctional cobalt sulfides for flexible supercapacitors and hydrogen evolution [J]. Journal of Materials Chemistry A, 2016, 4: 9014–9018.
- [24] WANG Q H, JIAO L F, DU H M, YANG J Q, HUAN Q N, PENG W X, SI Y C, WANG Y J, YUAN H T. Facile synthesis and superior supercapacitor performances of threedimensional cobalt sulfide hierarchitectures [J]. Cryst Eng Comm, 2011, 13: 6960–6963.
- [25] ZHANG L, WU H B, LOU X W D. Unusual CoS₂ ellipsoids with anisotropic tube-like cavities and their application in supercapacitors [J]. Chemical Communications, 2012, 48: 6912–6914.
- [26] ZHOU Y, JIN J, ZHOU X, LIU F, ZHOU P, ZHU Y, XU B. Cobalt sulfide@CNT-CNF for high-performance asymmetric supercapacitor [J]. Ionics, 2019, 25: 4031–4035.
- [27] CHEN Q, CAI D, ZHAN H. Construction of reduced graphene oxide nanofibers and cobalt sulfide nanocomposite for pseudocapacitors with enhanced performance [J]. Journal of Alloys and Compounds, 2017, 706: 126–132.
- [28] NADERI H R, SOBHANI-NASAB A, RAHIMI-NASRABADI M, GANJALI M R. Decoration of nitrogen-doped reduced graphene oxide with cobalt tungstate nanoparticles for use in high-performance supercapacitors [J]. Applied Surface Science, 2017, 423: 1025–1034.
- [29] AASHISH A, MOLJI C, PRIYA G K, SANKARAN M, NAIR U, HAREESH S, DEVAKI S J. Nanowires of polyaniline festooned silver coated paper electrodes for efficient solid-state symmetrical supercapacitors [J]. RSC Advances, 2018, 8: 33314–33324.
- [30] ANJANA P M, BINDHU M R, UMADEVI M, RAKHI R B. Antibacterial and electrochemical activities of silver, gold, andpalladium nanoparticles dispersed amorphous carbon

- composites [J]. Applied Surface Science, 2019, 487: 96-104.
- [31] LIU P, LIU J, CHENG S, CAI W, YU F, ZHANG Y, WU P, LIU M. A high-performance electrode for supercapacitors: Silver nanoparticles grown on a porous perovskite-type material La_{0.7}Sr_{0.3}CoO_{3-δ} substrate [J]. Chemical Engineering Journal, 2017, 328: 1–10.
- [32] ZOU Z, ZHOU W, ZHANG Y, YU H, HU C, XIAO W. High-performance flexible all-solidstate supercapacitor constructed by free-standing cellulose/reduced graphene oxide/silver nanoparticles composite film [J]. Chemical Engineering Journal, 2019, 357: 45–55.
- [33] RAHIMI-NASRABADI1 M, NADERI H R, KARIMI M S, AHMADI F, POURMORTAZAVI S M. Cobalt carbonate and cobalt oxide nanoparticles synthesis, characterization and supercapacitive evaluation [J]. Journal of Materials Science: Materials in Electronics, 2017, 28: 1877–1888.
- [34] ADIB K, RAHIMI-NASRABADI M, REZVANI Z, MAHDI POURMORTAZAVI S, AHMADI F, NADERI H R, GANJALI M R. Facile chemical synthesis of cobalt tungstates nanoparticles as high performance supercapacitor [J]. Journal of Materials Science: Materials in Electronics, 2016, 27: 4541–4550.
- [35] NAKANO M, FUJIWARA T, KOGA N. Thermal decomposition of silver acetate: Physico-geometrical kinetic features and formation of silver nanoparticles [J]. Journal of Physical Chemistry C, 2016, 120: 8841–8854.
- [36] DONG W, WANG X, LI B, WANG L, CHEN B, LI C, LI X, ZHANG T, SHI Z. Hydrothermal synthesis and structure evolution of hierarchical cobalt sulfide nanostructures [J]. Dalton Transactions, 2011, 40: 243–248.
- [37] SRIKESHG, SAMSON NESARAJ A. Chemical synthesis of Co and Mn co-doped NiO nanocrystalline materials as high-performance electrode materials for potential application in supercapacitors [J]. Ceramics International, 2016, 42: 5001–5010.
- [38] YIN P, SUN L, GAO Y, WANG S. Preparation and characterization of Co₉S₈ nanocrystalline and nanorods [J]. Bulletin of Materials Science, 2008, 31: 593–596.
- [39] KRISHNAMOORTHY K, VEERASUBRAMANI G K, KIM S J. Hydrothermal synthesis, characterization and electrochemical properties of cobalt sulfide nanoparticles [J]. Materials Science in Semiconductor Processing, 2015, 40: 781–786.
- [40] HUANG G. CHEN T, WANG Z, CHANG K, CHEN W. Synthesis and electrochemical performances of cobalt sulfides/graphene nanocomposite as anode material of Li-ion battery [J]. Journal of Power Sources, 2013, 235: 122–128.
- [41] TAO F, ZHAO Y Q, ZHAN G Q, LI H L. Electrochemical characterization on cobalt sulfide for electrochemical supercapacitors [J]. Electrochemistry Communications, 2007, 9: 1282–1287.
- [42] JOSHIA J H, KANCHAN D K, JOSHI M J, JETHVA H O, PARIKH K D. Dielectric relaxation, complex impedance and modulus spectroscopic studies of mix phase rod like cobalt sulfide nanoparticles [J]. Materials Research Bulletin, 2017, 93: 63-73.
- [43] MURADOV M B, BALAYEVA O O, AZIZOV A A, MAHARRAMOV A M, QAHRAMANLI L R, EYVAZOVA G M, AGHAMALIYEV Z A. Synthesis and characterization

- 2774 Alagu Segar DEEPI, Arputharaj Samson NESARAJ/Trans. Nonferrous Met. Soc. China 30(2020) 2764–2774
 - of cobalt sulfide nanoparticles by sonochemical method [J]. Infrared Physics and Technology, 2018, 89: 255–262.
- [44] RAMACHANDRAN R, FELIX S, SARANYA M, SANTHOSH C, VELMURUGAN V, RAGUPATHY B P C, JEONG S K, GRACE A N. Synthesis of cobalt sulfide– graphene (CoS/G) nanocomposites for supercapacitor applications [J]. IEEE Transactions on Nanotechnology, 2013, 12: 985–990.
- [45] DEEPI A, SRIKESH G, SAMSON NESARAJ A. Electrochemical performance of Bi₂O₃ decorated graphene nano composites for supercapacitor applications [J]. Nano-Structures & Nano-Objects, 2018, 15: 10–16.
- [46] DEEPI A, SRIKESH G, SAMSON NESARAJ A. One pot reflux synthesis of reduced graphene oxide decorated with silver/cobalt oxide: A novel nano composite materials for high capacitance applications [J]. Ceramics International, 2018, 44: 20524–20530.
- [47] ZHU J, ZHOU W, ZHOU Y, CHENG X, YANG J. Cobalt sulfide/reduced graphene oxide nanocomposite with enhanced performance for supercapacitors [J]. Journal of Electronic Materials, 2019, 48: 1531–1539.
- [48] RAMACHANDRAN R, SARANYA M, SANTHOSH C, VELMURUGAN V, RAGHUPATHY B P C, JEONG S K, GRACE A N. Co₉S₈ nanoflakes on graphene (Co₉S₈/G) nanocomposites for high performance supercapacitors [J]. RSC Advances, 2014, 4: 21151–21162.
- [49] JUSTIN P, RAO G R. CoS spheres for high-rate electrochemical capacitive energy storage application [J].

- International Journal of Hydrogen Energy, 2010, 35: 9709–9715.
- [50] ZHANG C, CAI X, QIAN Y, JIANG H, ZHOU L, LI B, LAI L, SHEN Z, HUANG W. Electrochemically synthesis of nickel cobalt sulfide for high-performance flexible asymmetric supercapacitors [J]. Advanced Science, 2017, 5: 1700375–1700387.
- [51] TAO F, ZHAO Y Q, ZHANG G Q, LI H L. Electrochemical characterization on cobalt sulfide for electrochemical supercapacitors [J]. Electrochemistry Communications, 2007, 9: 1282–1287.
- [52] SUN W, DU Y, WU G, GAO G, ZHU H, SHEN J, ZHANG K, CAO G. Constructing metallic zinc-cobalt sulfide hierarchical core-shell nanosheet arrays derived from 2D metal-organic- framework for flexible asymmetric supercapacitor with ultrahigh specific capacitance and performance [J]. Journal of Materials Chemistry A, 2019, 7: 7138-7150.
- [53] LIU Y, GUO S, ZHANG W, KONG W, WANG Z, YAN W, FAN H, HAO X, GUAN G. Three-dimensional interconnected cobalt sulfide foam: Controllable synthesis and application in supercapacitor [J]. Electrochimica Acta, 2019, 317: 551–561.
- [54] KUMAR Y A, RAO S S, PUNNOOSE D, TULASIVARMA C V, GOPI C V V M, PRABAKAR K, KIM H J. Influence of solvents in the preparation of cobalt sulfide for supercapacitors [J]. Royal Society Open Science, 2017, 4: 170427.

用于电化学超级电容器的性能优异的 六角形 Ag@CoS/rGO 纳米复合电极材料的设计

Alagu Segar DEEPI, Arputharaj Samson NESARAJ

Department of Applied Chemistry, School of Sciences, Arts, Media and Management, Karunya Institute of Technology and Sciences (Deemed to be University), Karunya Nagar, Coimbatore-641 114, Tamil Nadu, India

摘 要:合成混合金属/金属硫化物(Ag@CoS)与还原氧化石墨烯(rGO)的纳米复合材料(Ag@CoS/rGO),有可能用作超级电容器的电极。采用水热法成功地将 Ag@CoS 沉积在还原氧化石墨烯纳米片上,这意味着在还原氧化石墨烯骨架上生长出二维银和硫化钴基的六角形结构。对所合成的复合材料的结构、形貌和电化学行为进行研究。XRD结果表明,制备的纳米复合材料由于 CoS 和 Ag 的加入而呈六角结构。FTIR 光谱中出现在 470.33 cm⁻¹ 附近的谱带为 Ag@CoS/rGO 纳米复合材料中 S一S 键的吸收谱。采用扫描电镜(SEM)和透射电镜(TEM)分析材料清晰的六角结构,其晶粒尺寸从纳米级到微米级。该电极材料表现出良好的循环稳定性,当电流密度为 0.5 A/g 时,其比电容为 1580 F/g。即使经过 1000 次循环,容量保持率也没有任何损失。由电化学行为研究结果可知,所制备的新型纳米复合材料非常适合用作电化学超级电容器的电极。

关键词: Ag@CoS/rGO 电极; 水热反应; 物理化学特性; 电化学性能; 电化学超级电容器

(Edited by Wei-ping CHEN)